Automatic Detection and Classification of Ca2+ Release Events in Confocal Line- and Framescan Images

Ardo Illaste

Affiliation not available

Ernst Niggli

Affiliation not available

December 13, 2018

1 Introduction

Elementary Ca2+ signaling events occur in many different cell types and exhibit a variety of spatiotemporal features, according to which they were classified. For such events an ever growing nomenclature has been developed (e.g. Ca2+ sparks, puffs, blinks, quarks, etc., for review see Niggli, E., and N. Shirokova. 2007. A guide to sparkology: The taxonomy of elementary cellular Ca2+ signaling events. Cell Calcium. 42:379–387.). More complex Ca2+ signals, such as Ca2+ waves and whole-cell Ca2+ transients are often composed of a variable number of such elementary events.

Numerous methods exist for analysing Ca2+ sparks and other types of elementary and global Ca2+ signals in confocal linescan images. These employ various different approaches: noise tresholding [4, 3], wavelet transform [6], etc.

Recently, a method was developed by Tian et al., [7], where the fluorescence time trace in each pixel is fitted and provides a practically noise free approximation of the original fluorescence data. This pixel-by-pixel method had, however, several limitations which made it impractical to be used for Ca2+ release event detection.

Here we extend the method by Tian et al., in several ways. The new method allows for Ca2+ release event classification based on pixel-by-pixel denoising of the original signal.

2 Methods

2.1 Cell isolation

2.2 Solutions

2.3 Confocal Ca2+ imaging

Data acquisition was performed on two confocal setups. Linescan images were obtained on an Olympus FluoView 1000 confocal microscope. Framescan images were recorded with a VTInfinity multi-beam confocal microscope recording 512x64 pixel images at 150Hz freqency.

2.4 Computational

The detection algorithm is presented in the Results section.

3 Results

3.1 Pixel by pixel event classification

The algorithm is presented schematically on figure 1. Each subroutine is explained in detail below.

3.1.1 Region detection

Before it is possible to fit the fluorescence signal in each pixel with a transient function, candidate regions containing possible events must be detected. For this we have modified a continous wavelet transform based peak detection algorithm by Du et al.[2]. Whereas the the original algorithm of Du et al. provides the location of the peak, we have extended it to also yield the the width of the peak.

The original algorithm works by calculating a wavelet transform of the signal for increasing window lengths (Figure 1 B). Ridge lines along local maxima on the surface correspond to peaks if they satisfy certain criteria (length of the ridge, SNR, etc., see Du et al.[2] for details) In our extension, the width of the peak is obtained from finding the first maximum of the wavelet transform values along the ridge line (Figure 1C). The left and right edges of the region are taken as $[peak_{center} - 1.5 \times width, peak_{center} + 2 \times width]$

Region estimation provides a ranked list of potential event regions. The rank of a region indicates how many regions having a lower peak SNR overlap with it. For example, region 1 and 3 on Figure 1D have rank 3, because neither overlap with a region having a lower peak SNR. Region 2 has a rank of 2 as it overlaps with region 3 which has a lower peak SNR. Ranking is necessary to ensure overlapping signals are correctly fitted in the fitting stage.

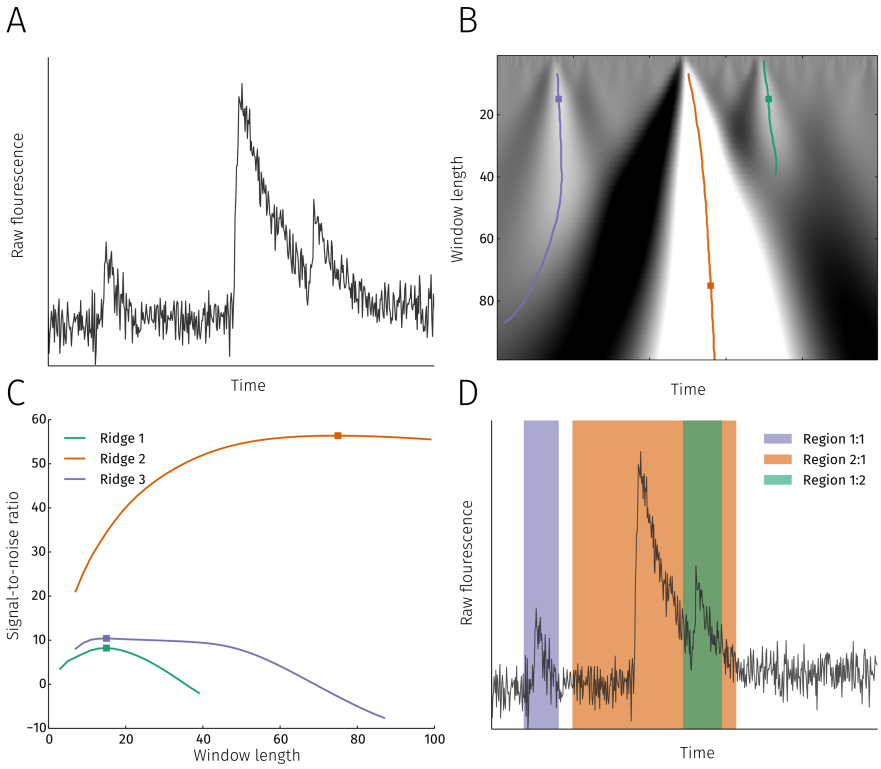

Figure 1: **Detecting regions with potential events. A** Example of a raw fluorescence signal from a single pixel for which event regions are detected. **B** Continous wavelet transform is perfomed on the raw signal with varying wavelet widths. Coloured lines indicate ridge lines along maxima at changing window length values. Squares denote the first maxima on each ridge line. **C** Signal-to-noise ratio of the continous wavelet transform along each ridge line. The first maximum on each ridge line is taken as the region size. **D** Regions detected by the algorithm.

3.1.2 Signal fitting

Fitting function for transients The function used for fitting Ca2+ release events is shown on Figure 3. The shape of the function is described by 4 parameters: amplitude (A), rise and decay time constants (τ_r, τ_d) and plateau duration (d). An additional parameter (μ) determines the time when the maximum is

reached. The function describing a transient is:

$$g(A, d, \tau_d, \tau_r, \mu, t) = A \cdot \begin{cases} 1 - \exp\left(-\frac{t-\mu}{\tau_r}\right) \cdot \exp(-2) & \mu - 2\tau_r \leq t < \mu \\ 1 - \exp(-2) & \mu \leq t < \mu + d \\ \exp\left(-\frac{t-\mu-d}{\tau_d}\right) \cdot (1 - \exp(-2)) & t \geq \mu + d \\ 0 & \text{otherwise} \end{cases} \tag{1}$$

The transient consists of four phases: zero level before the onset of the transient, an exponential increase with time constant τ_r starging when $t = \mu - 2\tau_r$, a plateau phase of duration d starting at $t = \mu$ and an exponential decay with time constant τ_d starting at $t = \mu + d$

For the optimizer to obtain good performance when fitting, the function used for fitting should be continously differentiable. With this in mind, the transient function is convolved with a gaussian $G(\sigma)$ to yield the actual fitting function:

$$f(A, d, \tau_d, \tau_r, \mu, t, \sigma) = g * G$$

For notational purposes we shall represent the fit function parameters by the vector

$$\mathbf{p} = \begin{bmatrix} A & d & \tau_d & \tau_r & \mu \end{bmatrix}$$

. The smoothing parameter σ will be fixed for all pixels. Therefore, for the i-th pixel the k-th event is represented by $f(\mathbf{p}_{i,k}, t)$.

The entire raw signal for the i-th pixel can be represented as:

$$F_i(t) = b(\mathbf{q}_i, t) + \sum_{k=0}^{m} f(\mathbf{p}_{i,k}, t) + W + R$$

, where b is a n-th order polynomial with $\mathbf{q}_i$ being the polynomial coefficients for the i-th pixel, summation is performed over all m events in the pixel, W represents noise and R is the remaining residual not captured in the baseline nor events. Ideally, $R = 0$, but achieving this is limited by the accuracy of the event region detection (we cannot fit what we do not detect) and whether or not our fitting function is general enough to be able to approximate various types of events.

Because it is not known which part of the signal is the event and which is the baseline, the first fit also has to estimate the baseline properties. Signal in the candidate region is fitted with an extended fit function (Figure 3) that also depends on relaxation baseline B and baseline offset C. The C parameter allows for the possibility of an elevated background before the release event.

Iterative fitting Fitting of potential event regions is performed iteratively. The algorithm is depicted on figure x.

First, the highest ranked regions are fitted with the extended fit function. After parameter optimization with the signal in the region is fitted with a linear model. For both models the corrected Akaike Information Criterion (AICc [1])

is calculated and the region is taken to contain an event only if the AICc for the fit function is less than the AICc for the line. This ensures that the fit obtained with the fit function is good enough to justify the use of the more complicated model. After this the fit is subtracted from the original signal. This allows the lower ranked regions to be fitted with reduced interference from higher ranking regions (see supporting info figures). When all regions have been fitted and their fits subtracted from the signal, the remaining signal is fitted with a polynomial function to approximate the baseline fluorescence.

In the second stage signals from approved regions are fitted again. Before performing the fit for each region, the baseline and previously obtained fits for other regions are subtracted from the raw signal. This allows the simpler fit function to be used as the subtraction eliminates the need for the extra baseline parameters (B and C). Once all regions are fitted in this manner the results are subtracted from the raw signal to estimate the baseline again. The second fitting stage is repeated once to improve the quality of the fits.

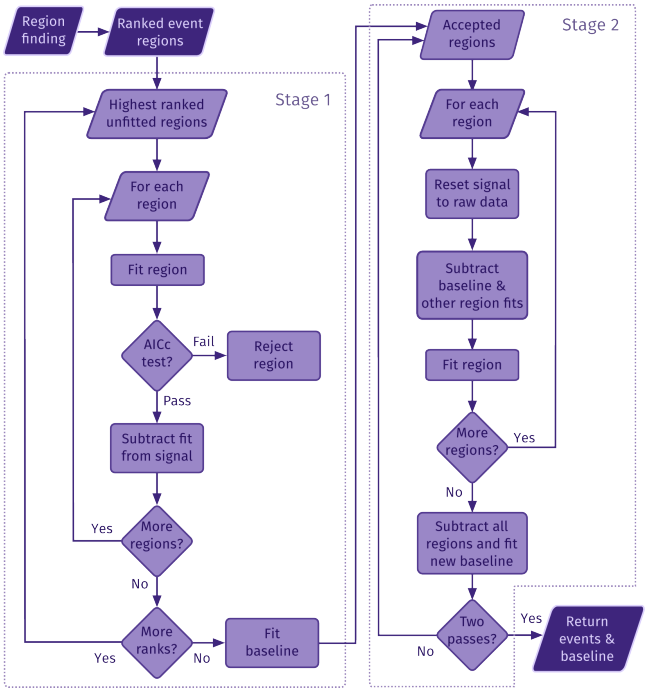

Figure 2: Diagram depicting the procedure for estimating parameters of events and overall baseline in detected regions.

Approximating the original image Having detected events from all the pixels it is possible to combine all fitted pixels into an approximation of the

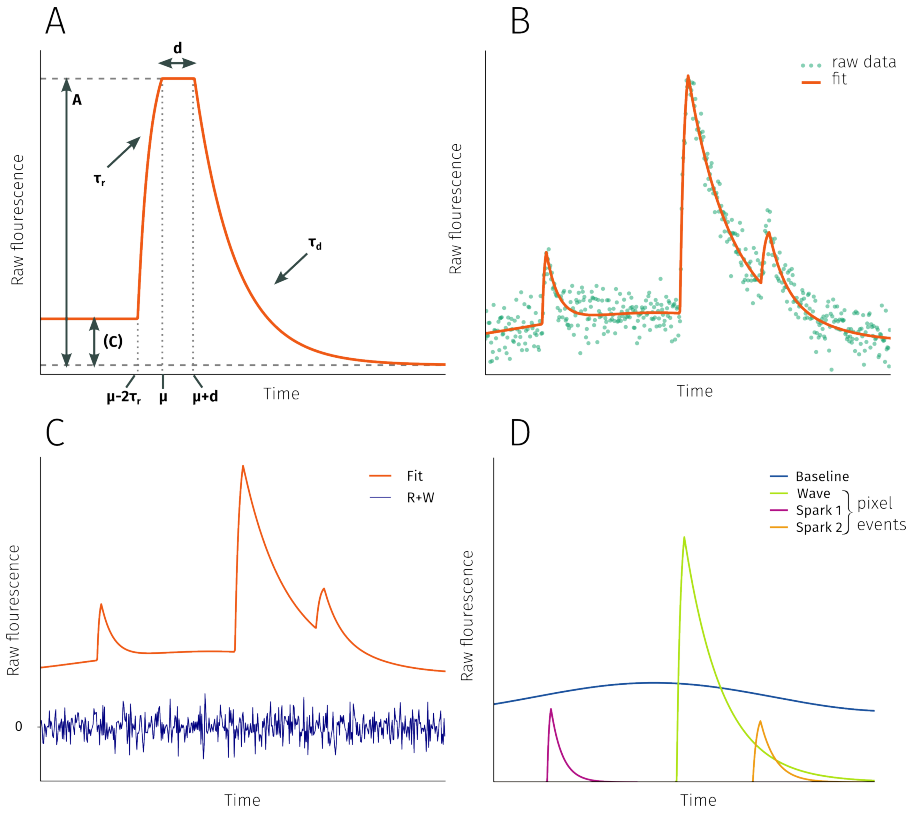

Figure 3: **Fitting function.** **A**: Fitting function for transients given by eq 1. **B** Result of fitting raw fluorescence data with the combined fitting function. **C** Raw signal is the sum of the fit, noise (W) and residual (R). **D** The fit is a superposition of the baseline and pixel events.

original image having a reduced level of noise. The results of applying the denoising algorithm to a linescan image, where one pixel corresponds to one horizontal line (Figure 4A), are presented on Figure 4B. The fitted image is obtained by adding the baseline image (Figure 4C) and fitted pixelevents (Figure 4D). Separating the baseline and events into separate images allows to easily calculate the standard $\Delta F/F_0$ image of the linescan (4E). Substracting the fitted image from the original data yields the noise and residual ($W + R$ in Eq. **??**). The histogram of the unfitted portion of the signal is symmetric around zero and gaussian.

Shape and location parameters Each pixel event is characterized by the parameters $\mathbf{r}$. Four of these (A, d, τ_d, τ_r) determine the shape of the event and μ the location in time. In order to completely charactarize a pixel event it is also

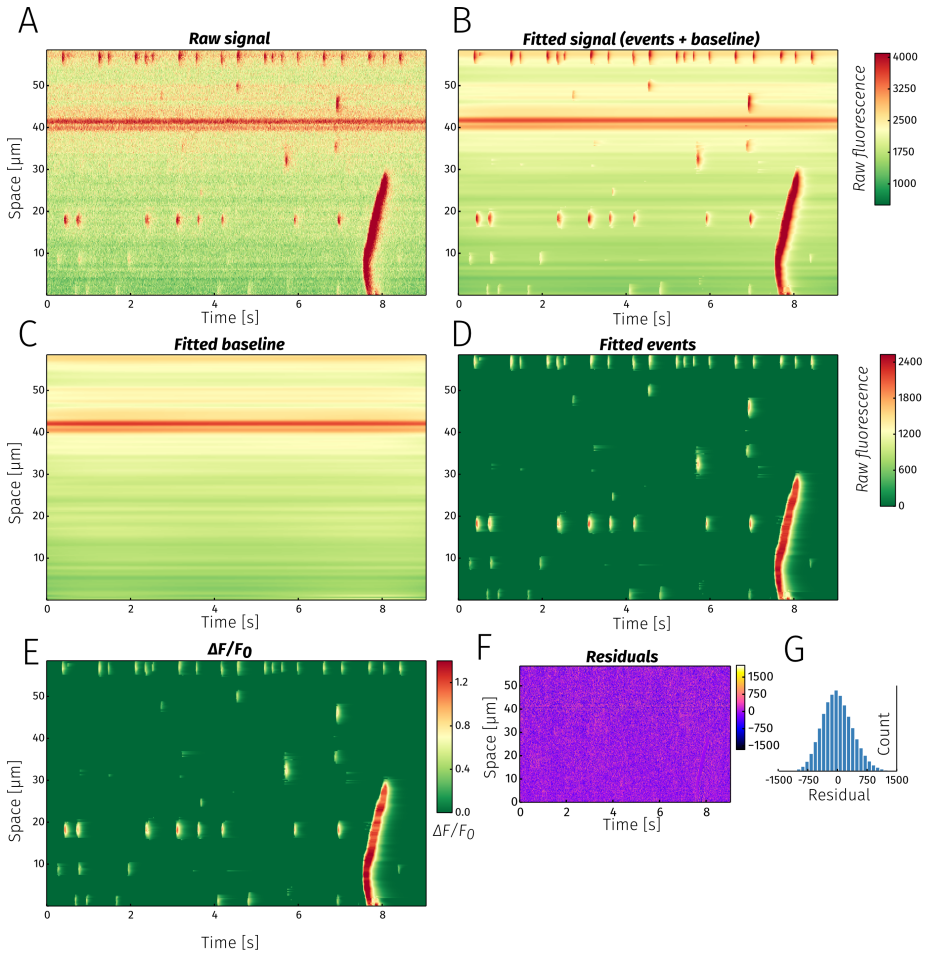

Figure 4: **Fitting a linescan image.** **A** Raw fluorescence signal. **B** Each horizontal line along the temporal axis was fitted with the fitting algorithm. The fitted signal in the denoised image is a sum of fitted events (**C**) and baseline (**D**). ΔF/F0 image (**E**) is obtained by dividing the event image (**C**) with the baseline (**D**). Because the fitted baseline is a function of time, the ΔF/F0 image is automatically corrected for temporal changes in background fluorescence (e.g., bleaching). **F** The residual signal obtained when subtracting the fitted image from raw data. **G** Histogram of the residual values.

necessary to know the pixel's spatial location. This would require one or two spatial coordinates, respectively for line- or framescans. Hence, a pixel event is wholly defined by two vectors: the shape parameter vector $\mathbf{p}^s = [A, d, \tau_d, \tau_r]$ and the position parameter vector $\mathbf{p}^p = [\mu, x, y]$.

The k-th event detected in pixel i is represented by vectors $\mathbf{p}^s_{i,k}$ and $\mathbf{p}^p_{i,k}$. An event matrix for the i-th pixel E_i contains the parameter vectors for all the events in the pixel:

$$E_i = \begin{pmatrix} \mathbf{p}^s_{i,0} & \mathbf{p}^p_{i,0} \\ \mathbf{p}^s_{i,1} & \mathbf{p}^p_{i,1} \\ \cdots & \\ \mathbf{p}^s_{i,k} & \mathbf{p}^p_{i,k} \end{pmatrix} = \begin{pmatrix} E^s_i & E^p_i \end{pmatrix}$$

The event matrix for the entire image is obtained by stacking all pixel event matrices:

$$E = \begin{pmatrix} E_0 \\ E_1 \\ \vdots \\ E_i \end{pmatrix} = \begin{pmatrix} E^s_0 & E^p_0 \\ E^s_1 & E^p_1 \\ \vdots & \vdots \\ E^s_i & E^p_i \end{pmatrix} = \begin{pmatrix} E^s & E^p \end{pmatrix}$$

, where E^s and E^p are shape and position submatrices, respectively, containing event shape and position parameters for all events from all pixels and making up the entire image event matrix E. The separation of shape and position parameters for events is necessary in the next clustering step.

3.1.3 Clustering

Having determined the events in each pixel it is possible to reconstruct the image with reduced noise levels using the matrix E. However, this will not tell us anything about the properties of actual release events (e.g., spark/wave numbers or properties) as these macroscopic events are made up of several events from different pixels. It is therefore necessary to combine elementary events from various pixels into macroscopic release events.

This is achieved using the clustering method DBSCAN [5]. The algorithm? works in the parameter space and finds clusters of arbitrary shape based on the density of events. In contrast to many other clustering methods (e.g., k-nearest neighbours, spectral clustering) the number of clusters found is not determined in advance. The number of clusters found depends on the data and two parameters: minimum number of events in a cluster and the maximum distance from a cluster to be included in it).

Clustering is performed in two steps. First, pixel events are distributed into groups according to their shape i.e., clustering is done on the matrix E^s. This is possible because, although the function used for fitting various release events (e.g., sparks or waves) is the same, the shape parameters of a event

approximating a spark are likely to be more similar to other spark events rather than wave events. This is clearly visible on Figure 4A where ...

In the second clustering step, the E^p matrix is processed for each shape group and clusters of spatiotemporally close events are obtained. An example of results of this positional clustering is shown on Figure 4B where events making up single sparks are depicted in various shades of orange. A single wave is shown in blue. Events that failed to be classified are black. Events that fail to be classified in either the shape or positional clustering steps are essentially filtered out as invalid events. With this two-step approach, release events of various types consisting of elementary events from multiple pixels are obtained.

3.1.4 Algorithm parameters

3.1.5 Event characterisation

linescan sparks + wave / restitution
    linescan sr waves
    framescan

3.2 Sensitivity analysis

3.2.1 Pixel trace

As the amount of noise in the signal increases the performance of the event detection algorithm should decrease (Fig X A). The sensitivity of the method to noise was explored by estimating both the probability of detecting an event in a noisy signal and the accuracy of the fit. The original signal to be fitted was generated from the fitting function for five different amplitudes. To this signal different levels of normally distributed noise was added (noise level is the standard deviation of the noise distribution). Figure x B shows the probability of detecting the event in the signal as a function of noise level. Increasing the event amplitude shifts the event detection probability curve towards higher noise levels and vice-versa. It is more informative to look at the relationship between detection probability and the signal to noise ratio of the event. This is calculated as:

$$SNR = \frac{\int_a^b f(t)^2\, dt}{(b-a)\,\sigma_n^2}$$

where a and b are times, before and after the peak respectively, when the fluorescence is at half of its peak value (i.e., b-a is FDHM), *f(t)* is the event signal and σ_n the standard deviation of the noise (i.e., noise level). The resulting plot is depicted on figure x C, and it can be seen that detection probability is only dependent on the *SNR*. For visual comparison, the appearance of 4 events with different *SNR* and detection probabilities are shown on Figure x.

On Figure X D the accuracy of the fit compared to the original event is estimated for various amplitudes and noise levels as the R^2 value. Predicatably

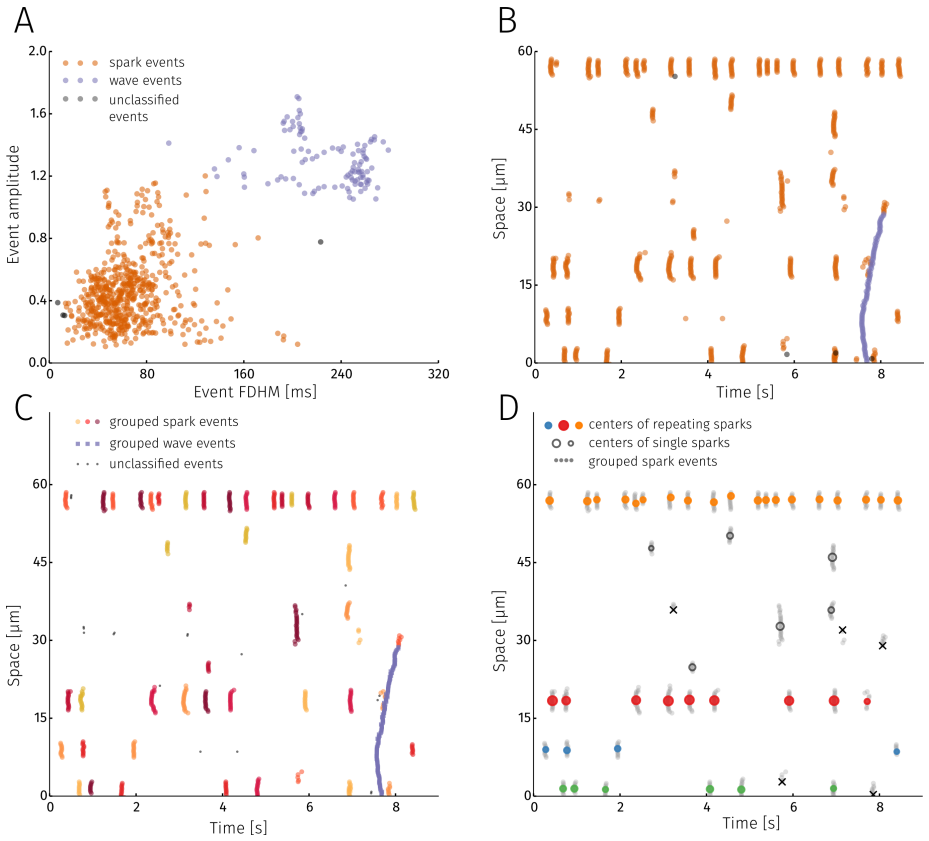

Figure 5: **Classifying detected events.** **A** Density based clustering algorithm is used to classify pixel events into categories based on their shape. Colours represent event categories. Black signifies events which could not be categorized. **B** Categories obtained from clustering by shape plotted according to event location. **C** In the second step of classification each shape category is clustered further based on location. Groups of pixel events are obtained that make up a Ca2+ release even (in this case sparks and a wave). **D** All detected sparks visualized according to their center(location of coloured circle) and amplitude (colour of the circle). Events marked with a black x were not symmetric and not classified as sparks. Circle colour shows sparks originating from the same 2um segment. Empty circles are sparks with no nearby sparks.

the R^2 value decreases as the amount of noise increases. Again, the R^2 curves calculated for different amplitudes overlap when plotted as a function of *SNR*. Combining plots XC and XE the relationship between the probability of finding an event and the accuracy of the fit can be obtained.

3.2.2 Release event detection

3.3 Biological results

3.3.1 Spark location and parameters

Locations of individual sparks can be estimated once the clustering steps are done. The fluorescence image for each spark is reconstructed from all its pixel events. A gaussian is fitted to the spatial profile of the spark at the time of maximum fluorescence. The spatial location and FWHM are obtained from the fit parameters.

3.3.2 Waves in the cytosol and SR

When analyzing Ca2+ waves in cardiomyocytes it is customary to deskew them (REF) before averaging the signal in the spatial dimension. This relies on detecting the half maximal fluoresence along each pixel and then straigthening the linescan. This approach can be problematic in case of noisy images or when dealing with several waves in one image. With our method deskewing the linescan is not necessary. The peak time for each pixelevent composing the wave will be known from fitting and can be used to calculate the average wave profile and wave speed. It is also possible to use detected cytosolic wave events to analyze Ca2+ waves in the sarcoplasmic reticulum (SR). The SR signal is more noisy than the cytosolic which makes it difficult to apply the fitting algorithm directly. Assuming that a decrease in the SR signal is accompanied by increased flourescence in the cytosol, the first step of the algorithm - region detection - can be skipped and the regions detected in the cytosol reused for analysis in the SR.

Homogeneinity of release (REF to nina)

3.3.3 Framescan analysis

Despite having focused on analysing linescans so far, the method can be readily applied to analysis of framescans as well. Figure X shows the results for framescan analysis, comparing raw, fitted and delta F images from the same 139x33 pixel area (X x Y um). For each case three different timepoints are presented: a wave, a weak spark and a strong spark.

Event clustering for framescan images is performed in a similar fashion to linescan images, with the exception of two spatial dimensions used for release event grouping.

The information provided by the method parameter maps can be constructed for release events. On Figure examples of wave maximum time, angle and speed are shown.

4 Discussion

This project was supported by a SciEx felloship (to A.I.) and by Swiss National Science Foundation grants (31-132689 and 31-156375 to E.N.). We would like to thank M. Courtehoux for expert technical assistance.

5 Appendix

5.0.1 Image preprocessing

The only preprocessing step used is convolving the image with a $(2n+1)\times(2n+1)$ kernel where the center element is $1/(n+1)$ and the k-th layer surrounding the center is made up of values $1/(8k \cdot (n+1))$. For example, when n=1 the kernel would be

$$\begin{pmatrix} {}^1/_{16} & {}^1/_{16} & {}^1/_{16} \\ {}^1/_{16} & {}^1/_{2} & {}^1/_{16} \\ {}^1/_{16} & {}^1/_{16} & {}^1/_{16} \end{pmatrix}$$

Convolving the image with this kind of kernel reduces the noise while retaining more of the original signal than simple averaging. Contributions from the i-th layer around the center will have the same weight as the central pixel. In this work we use the kernel with $n = 1$.

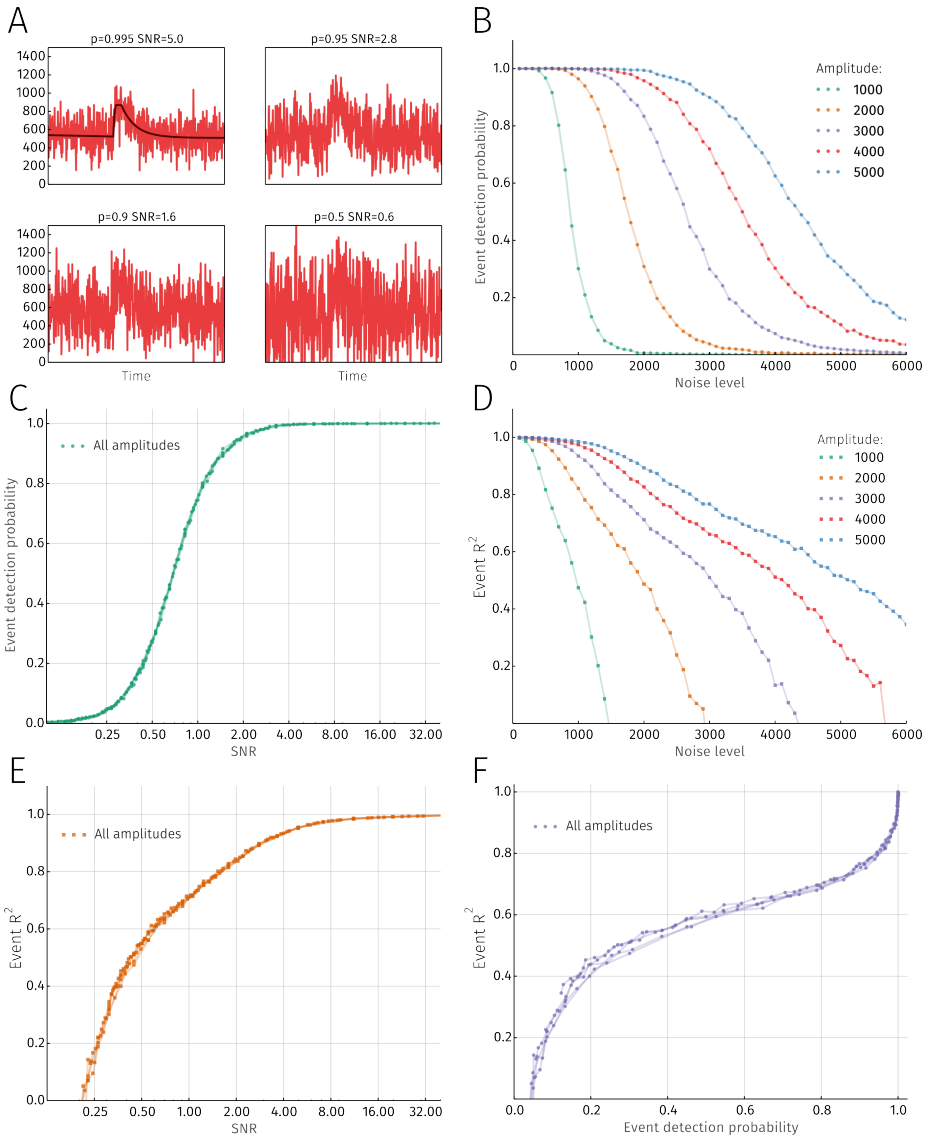

Figure 6: **Sensitivity and accuracy of the algorithm.** **A** Four version of the same original signal (shown in black on the top left panel) with different levels of added noise. The title for each plot indicates detection probability and the signal to noise ratio (SNR) for the each respective signal. **B** Detection probabilities as a function of noise level for signals with various amplitudes. **C** Detection probabilities as a function of SNR are no longer dependent on signal amplitude. **D** R2 value for detected events as a function of noise level for signals with various amplitudes. **E** R2 value as a function of SNR. **F** Combining (**C**) and (**E**) to show the relationship between detection probability and fit accuracy.

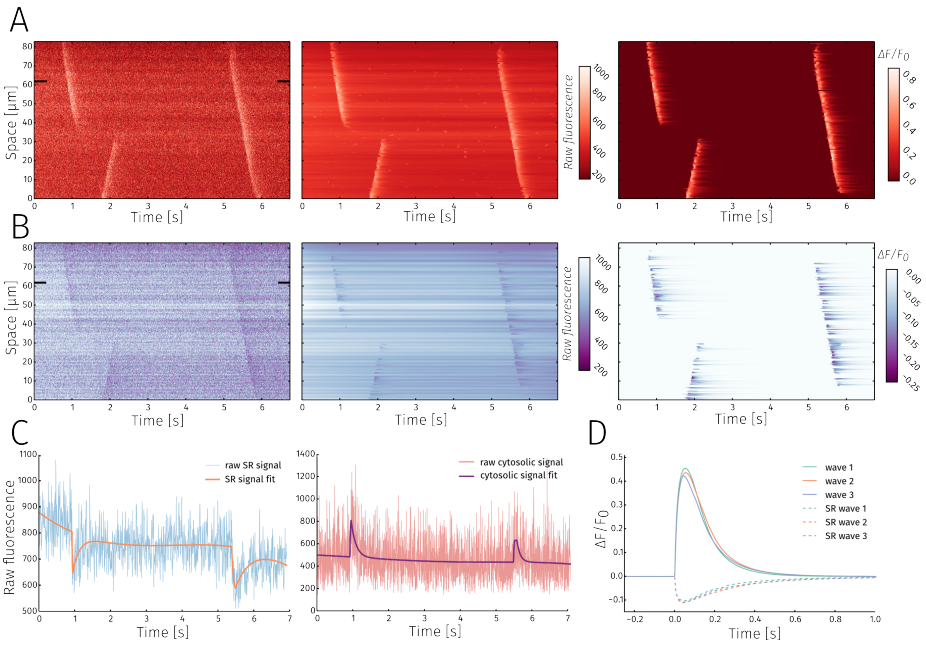

Figure 7: **Dual channel linescan analysis A** and **B** show, from left to right, the raw signal, fitted signal and DF/F0 for cytosolic and SR measurements, respectively. **C** Raw data with the fit for a time trace from a single pixel(indicated by black rectangles on (**A**) and (**B**)) for SR(left) and cytosolic(right) signals. **D** Average wave profiles for the 3 detected waves in SR and cytosol.

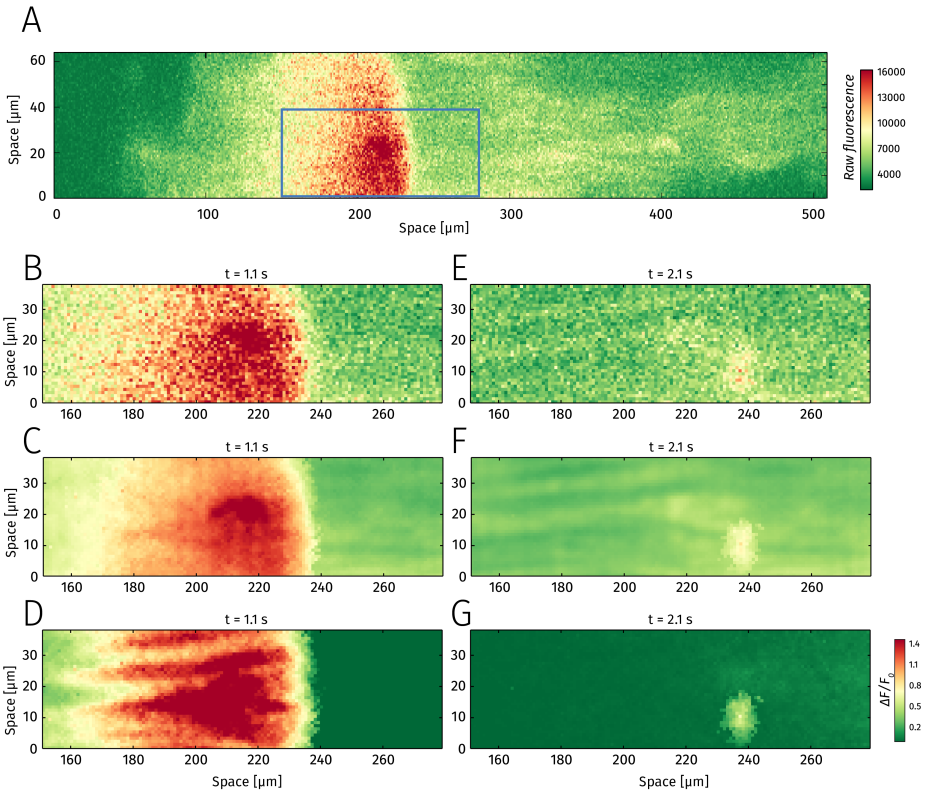

Figure 8: **Framescan analysis A** Snapshot of a 512x64 pixel framescan at t=1.1 seconds after initiation of recording. Rectangle shows the in focus region analyzed in subsequent panels. **B, C, D** Raw image, pixel-by-pixel fitted image and $\Delta F/F_0$, respectively for a Ca2+ wave. **E, F, G** Raw image, pixel-by-pixel fitted image and $\Delta F/F_0$, respectively for a Ca2+ spark.

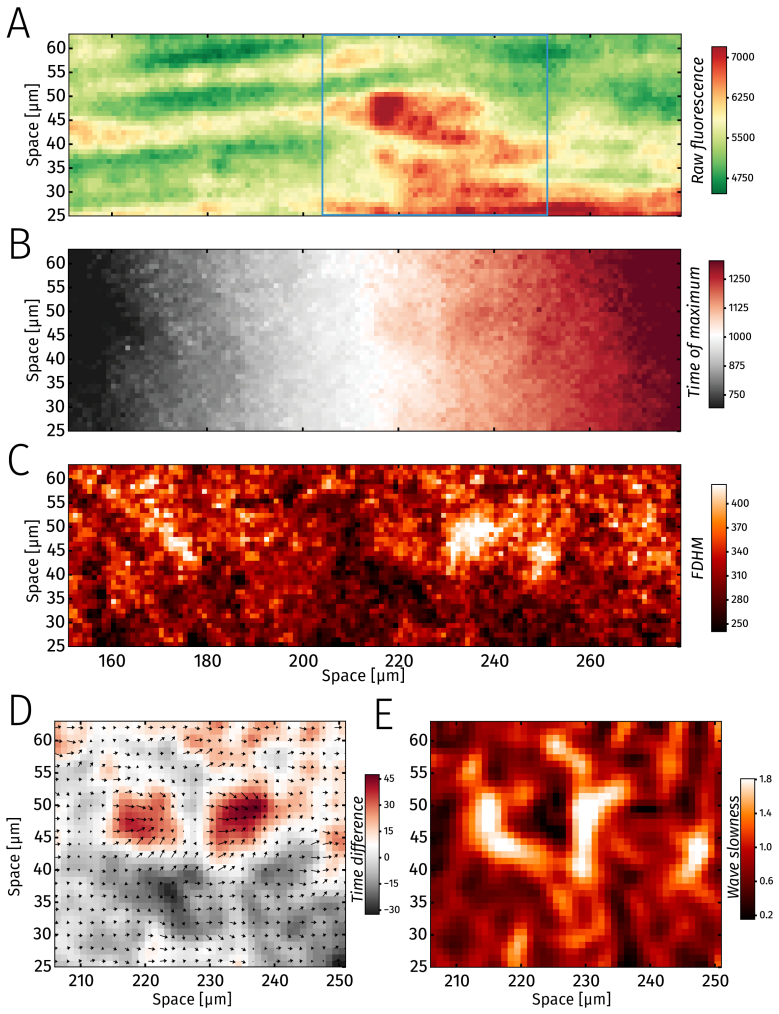

Figure 9: **Detailed framscan analysis A** Baseline fluorescence (dye distribution) in the zoomed in region from Figure 8. **B** Map showing wave peak time. **C** Map showing wave FDHM **D** Time difference between actual time of wave maximum and expected time. Arrows indicate the gradient of wave peak time. **E** Wave slowness - i.e., highest resistance to wave traversal.

References

[1] K. P. Burnham. Multimodel Inference: Understanding AIC and BIC in Model Selection. *Sociological Methods and Research*, 33(2):261–304, Nov 2004.

[2] P. Du, W. A. Kibbe, and S. M. Lin. Improved peak detection in mass spectrum by incorporating continuous wavelet transform-based pattern matching. *Bioinformatics*, 22(17):2059–2065, Sep 2006.

[3] E. Picht, A. V. Zima, L. A. Blatter, and D. M. Bers. SparkMaster: automated calcium spark analysis with ImageJ. *AJP: Cell Physiology*, 293(3):C1073–C1081, Jun 2007.

[4] E. Ríos, N. Shirokova, W.G. Kirsch, G. Pizarro, M.D. Stern, H. Cheng, and A. González. A Preferred Amplitude of Calcium Sparks in Skeletal Muscle. *Biophysical Journal*, 80(1):169–183, Jan 2001.

[5] Jörg Sander, Martin Ester, Hans-Peter Kriegel, and Xiaowei Xu. *Data Mining and Knowledge Discovery*, 2(2):169–194, 1998.

[6] László Zsolt Szabó, János Vincze, László Csernoch, and Péter Szentesi. Improved spark and ember detection using stationary wavelet transforms. *Journal of Theoretical Biology*, 264(4):1279–1292, Jun 2010.

[7] Q. Tian, L. Kaestner, and P. Lipp. Noise-Free Visualization of Microscopic Calcium Signaling by Pixel-Wise Fitting. *Circulation Research*, 111(1):17–27, Jun 2012.